IOPscience iopscience.iop.org

Home Search Collections Journals About Contact us My IOPscience

Giant magnetoresistance effect realized by depositing nanosized ferromagnetic and Schottky stripes on a semiconductor heterostructure

This article has been downloaded from IOPscience. Please scroll down to see the full text article.

2008 J. Phys.: Condens. Matter 20 335221

(http://iopscience.iop.org/0953-8984/20/33/335221)

View the table of contents for this issue, or go to the journal homepage for more

Download details:
IP Address: 129.252.86.83
The article was downloaded on 29/05/2010 at 13:55

Please note that terms and conditions apply.

IOP PUBLISHING JOURNAL OF PHYSICS: CONDENSED MATTER

J. Phys.: Condens. Matter **20** (2008) 335221 (5pp) doi:10.1088/0953-8984/20/33/335221

Giant magnetoresistance effect realized by depositing nanosized ferromagnetic and Schottky stripes on a semiconductor heterostructure

Gui-Lian Zhang[1,2], **Mao-Wang Lu**[1,2,3], **Yi Tang**[1] **and Sai-Yan Chen**[1,2]

[1] Faculty of Materials and Optoelectronic Physics, Xiangtan University, Xiangtan, Hunan 411105, People's Republic of China

[2] Department of Electronic Engineering and Physics, Hunan University of Science and Engineering, Yongzhou, Hunan 425100, People's Republic of China

E-mail: maowanglu@126.com

Received 28 January 2008, in final form 3 July 2008
Published 31 July 2008
Online at stacks.iop.org/JPhysCM/20/335221

Abstract

We propose a giant magnetoresistance (GMR) device by depositing nanosized ferromagnetic (FM) and Schottky normal metal (SM) stripes on the top of the GaAs heterostructure. It is shown that this device possesses a considerable GMR effect, whose magnetoresistance (MR) ratio can be up to $10^6\%$ at a certain energy. It is also shown that the MR ratio depends strongly on the structural parameters and the electrical barrier height induced by the applied voltage to the SM stripe, and thus this device can be used as a tunable GMR device.

1. Introduction

The giant magnetoresistance (GMR) effect was independently discovered by Fert *et al* [1] and Grunberg *et al* [2] in 1988. It has opened the door to a new field of science, magnetoelectronics (or spintronics), where two fundamental properties of the electron, namely its charge and its spin, are simultaneously manipulated. It has also given rise to a tremendous impact on magnetic information storage [3]. Fueled by its fascinating applications such as ultrasensitive magnetic field sensors, read heads and random access memories, thousands of scientists all around the world are today working on the magnetoelectric phenomena and their exploration. The structure where the GMR effect is observed usually consists of two ferromagnetic layers separated by a thin nonmagnetic layer. In such a heterogeneous system, GMR is characterized by a striking drop of electrical resistance when an external magnetic field switches the magnetization of adjacent magnetic layers from an anti-parallel (AP) alignment to a parallel (P) one. The degree of the GMR effect is usually characterized by the magnetoresistance ratio defined as $\mathrm{MR} = (G_\mathrm{P} - G_\mathrm{AP})/G_\mathrm{AP}$ or $(G_\mathrm{P} - G_\mathrm{AP})/G_\mathrm{P}$, where G_P and G_AP are the conductance for P and AP alignments, respectively. Usually, one hopes from the viewpoint of practical applications that the system possesses a high MR ratio under a relatively low saturation magnetic field.

Recently, hybrid ferromagnet/semiconductor devices have attracted a great deal of interest [4–6]. Theoretical developments have focused on the energy spectrum and transport properties, for example, wavevector filtering [7], spin polarized transport [8], energy spectrum and spin splitting [9], magnetoresistance [10], etc. Experimentally, the device could be realized by depositing magnetic or superconducting microstructures on the surface of a heterostructure with a two-dimensional electron gas (2DEG) using modern nanolithography. Microstructural ferromagnets or superconductors provide an inhomogeneous magnetic field which influences locally the motion of the electrons in the semiconductor. Nogaret *et al* [11] demonstrated an MR effect in such a device at low temperature, and a ratio up to $10^3\%$ at 4 K has been observed recently [12]. It was also reported that MR oscillations, due to the internal Landau band structure of a 2DEG system, can be observed in a periodic magnetic field [13].

[3] Author to whom any correspondence should be addressed.

 © 2008 IOP Publishing Ltd Printed in the UK

Generally, it seems that the spin-dependent transport is indispensable for the observation of the GMR effect. However, in 2002 Zhai *et al* [14] proposed a GMR device based on a δ-barrier magnetic nanostructure, which makes no use of the spin freedom of the electrons and possesses very high MR ratio at zero average magnetic field. The spin-independent GMR effect has since attracted considerable attention in this kind of magnetic barrier nanosystem [15–19]. The GMR effect in a realistic case, where the exact magnetic profiles instead of the ideal δ-function magnetic barriers were employed, was also studied by Lu *et al* [15]. Yang *et al* [16] investigated the GMR effect of a 2DEG system subjected to a periodically modulated magnetic field and found that the MR ratio of such a periodically modulated system shows strong dependence on the number of periods as well as the space between the magnetic barriers. The temperature dependence of the GMR effect in magnetic barrier nanostructures was also investigated by Papp *et al* [17].

Very recently, Papp *et al* [18] and Lu *et al* [19] proposed two novel GMR devices by depositing two ferromagnetic (FM) stripes on the top and the bottom of the GaAs heterostructure, respectively. In this paper, we propose a GMR device by the deposition of two FM stripes and a Schottky-metal (SM) stripe on the top of a conventional GaAs heterostructure. We have revealed that the proposed device possesses a considerable GMR effect and its MR ratio shows a strong dependence on the structural parameters and the electrical barrier height.

2. Model and method

The considered system is a 2DEG in the (x, y) plane subject to modulations of two FM stripes and an SM stripe as schematically depicted in figure 1(a), which can be realized experimentally by modern nanotechnology [20]. When a magnetic field is directed parallel to the 2DEG, the ferromagnetic materials become magnetized parallel to the 2D plane and the fringing field near the edge of the magnetic materials constitutes a non-homogeneous magnetic barrier perpendicular to the 2DEG. Each FM stripe induces a positive B_z underneath one edge and a negative B_z underneath the other edge. A suitable external magnetic field can change the relative orientation of the two magnetizations, which is anti-parallel at zero field. The SM stripe induces an electric barrier $U(x)$. The two FM stripes and the SM stripe are assumed to be parallel in figure 1(a). For simplicity, the magnetic and electric barriers can be approximated as a delta function and a square, respectively, in order to demonstrate the principle of operation of this device, as shown in figures 1(b) and (c). Here, figures 1(b) and (c) correspond to the parallel (P) and anti-parallel (AP) configurations of two FM stripes. The magnetic field can be written as

$$B_z(x) = B l_{B_0}\{[\delta(x) - \delta(x-d)] + \gamma\,[\delta(x-2D-2d) - \delta(x-2D-3d)]\}. \quad (1)$$

Here B gives the strength of the magnetic field, $l_{B_0} = \sqrt{\hbar/eB_0}$ is the magnetic length for the estimated magnetic field B_0, D is the space between two stripes, d is the width of the strips and γ represents the magnetization configuration

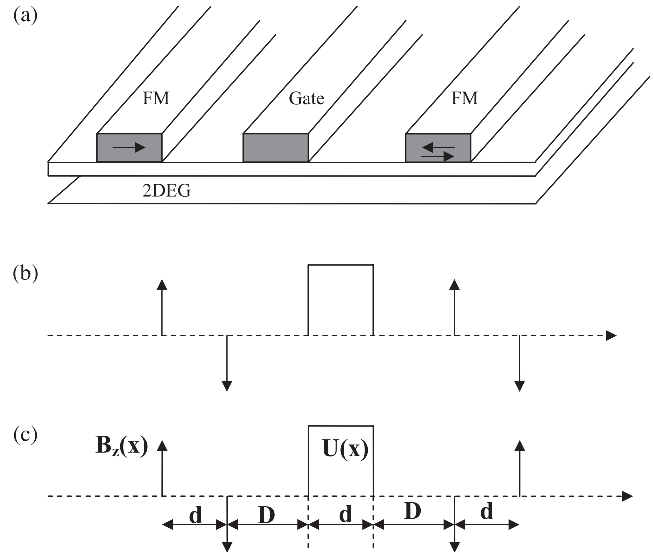

Figure 1. (a) Schematic illustration of the device and the model magnetic field profile for the parallel (b) and anti-parallel (c) configurations of two magnetic moments.

(± 1 or P/AP). Assume that the magnetic field provided by the FM stripes and the electric potential induced by the SM stripe are homogeneous in the y direction and only vary along the x axis. The motion of an electron in such a modulated 2DEG system in the (x, y) plane can be described by the single-particle Hamiltonian

$$H = \frac{[P + eA(x)]^2}{2m^*} + U(x) + \frac{g^*\mu_B B_z(x)\sigma_z}{2}, \quad (2)$$

where m^* is the effective mass, e is the absolute value of the electron's charge, μ_B is the Bohr magneton, g^* is the effective Landé factor of the electron in the 2DEG, $\sigma_z = +1/-1$ for spin up/down electrons, and the magnetic vector potential, in the Landau gauge, can be written as $\vec{A}(x) = [0, A_y(x), 0]$. Using the cyclotron frequency $\omega_c = eB_0/m^*$ and magnetic length l_{B_0}, all quantities could be expressed in dimensionless units, for example, the magnetic field $B_z(x) \to B_0 B_z(x)$, the magnetic vector potential $A(x) \to B_0 l_{B_0} A(x)$, the coordinate $x \to l_{B_0} x$, the wavevector $k \to l_{B_0}^{-1} k$ and the energy $E \to \hbar\omega_c E$ ($E_0 E$). In our calculation, we typically take for GaAs $n_e = 10^{11}$ cm^{-2} which gives $E_F = 3.55$ meV and we use $B_0 = 0.1$ T, which leads to the units $l_{B_0} = 81.3$ nm and $E_0 = 0.17$ meV for the GaAs system with $m^* = 0.067 m_0$ (m_0 is the free electron mass) and $g^* = 0.44$.

Because of the translational invariance of the system along the y direction, the total electronic wavefunction can be written as a product $\Phi(x, y) = e^{ik_y y}\Psi(x)$, where k_y is the transverse wavevector. $\Psi(x)$ satisfies the following reduced one-dimensional Schrödinger equation:

$$\left\{\frac{d^2}{dx^2} - \left[k_y + A_y(x)\right]^2 + 2\left[E - U(x) - \frac{m^* g^* \sigma_z}{4m_0} B_z(x)\right]\right\}\psi(x) = 0. \quad (3)$$

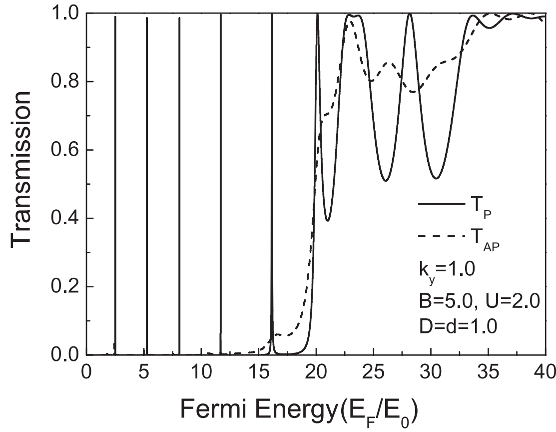

Figure 2. The transmission probability through a magnetic–electric barrier with parallel and anti-parallel magnetization as a function of energy for $k_y = 1.0$. The structural parameters are $B = 5.0$, $U = 2.0$, $D = d = 1.0$.

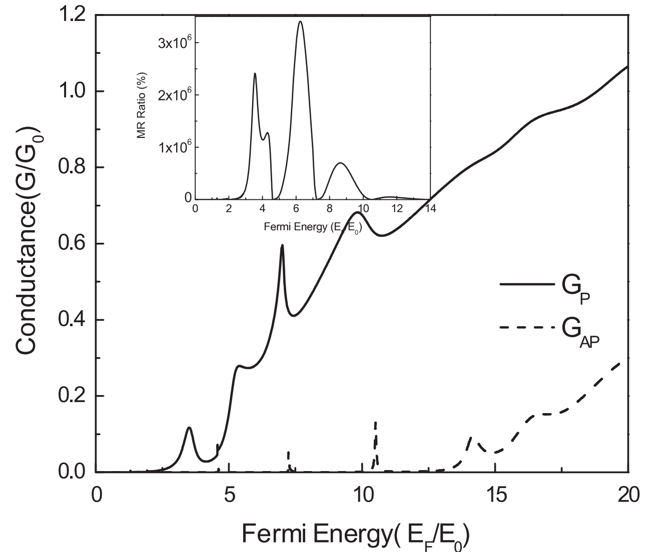

Figure 3. The conductance of electrons as a function of the Fermi energy for both P and AP alignments, where the structural configuration and its parameters are the same as in figure 2. The MR ratio as a function of Fermi energy is given in the insets for the same parameters.

It is going to be useful to introduce the effective potential of the magnetic–electric barrier:

$$U_{\text{eff}} = \tfrac{1}{2}\left[k_y + A_y(x)\right]^2 + U(x) + m^* g^* \sigma_z B_z(x)/4m_0. \quad (4)$$

The last term represents the Zeeman coupling between the electronic spin and the local magnetic field. As the absolute value of such a term is very small (even for $B/B_0 = 5$, the value of $m^* g^* B/4m_0$ is 0.0369 for GaAs) compared to other terms in U_{eff} and plays a minor role in determining the transport properties of the electrons [19], it will be omitted in the subsequent discussion [18]. Clearly, the effective potential of the system not only depends on the wavevector k_y but also on the configuration of the magnetic field. The k_y dependence renders the motion an essentially two-dimensional process. From the dependence of the U_{eff} on the magnetic profile $B_z(x)$, one can easily see that, for the device presented in figure 1, U_{eff} varies substantially when the P alignment turns to its inverse. It is the U_{eff} dependence on the magnetic profile that leads to the GMR effect in the involved system.

We adopt the transfer-matrix method to evaluate the transmission coefficient $T_\gamma(E, k_y)$ ($\gamma = \pm 1$ for P/AP). Furthermore, the ballistic conductance at zero temperature can be calculated by averaging the electron flow over half the Fermi surface from the well-known Landauer–Buttiker formula, and is given as the following [21]:

$$G_\gamma(E_{\text{F}}) = G_0(E_{\text{F}}) \int_{-\pi/2}^{\pi/2} T_\gamma(E_{\text{F}}, \sqrt{2E_{\text{F}}}\sin\varphi)\cos\varphi \, \mathrm{d}\varphi, \quad (5)$$

where φ is the angle of incidence relative to the x direction and the conductance is presented in units of $G_0(E_{\text{F}}) = 2e^2 m^* v_{\text{F}} L_y/h^2$,where L_y is the length of the structure in the y direction and v_{F} is the Fermi velocity.

3. Results and discussion

First of all, we plot the transmission coefficients in figure 2 for P and AP alignments versus the Fermi energy. The structural parameters are set to be $k_y = 1.0, B = 5.0$, $U = 2.0$ and $D = d = 1.0$. Apparently, there exists a remarkable discrepancy in the transmission for electrons tunneling through P and AP configurations of the FM layers, which is due to the strong dependence of the effective potential U_{eff} of the device on the magnetic configuration. For the P configuration, the transmission shows obvious oscillations and there exist several line-shaped resonant peaks with values of unity in the low-energy region. This can be expected because, for the considered wavevector k_y and electric potential U which is induced by the applied voltage to the SM stripe, the effective potential U_{eff} has a relatively symmetric multiple-barrier quantum-well structure for the P configuration, where the process of electron motion resonantly tunnels through the barrier when the incident energy coincides with one of the quasibound energy levels within the wells. However, when the system switches from the P configuration to the AP configuration, one can see that the electron transmission is greatly suppressed and the low-energy resonant peaks almost disappear. This is because, for the AP alignment, the effective potential U_{eff} has an non-symmetric multiple-barrier quantum-well structure, which makes electronic transmission through this alignment incomplete.

Having seen the configuration-dependent transmission features, now we see to what extent such a difference is reflected in the measurable quantity, the conductance G, which is obtained by integration of the transmission of electrons over the incident angle: cf equation (5). In figure 3, we present the conductance G_{P} and G_{AP} for the P and AP alignments versus the Fermi energy E_{F}, where the structural parameters are exactly the same as in figure 2 and the conductance is in units of G_0. In the low-energy region, the electronic transmissions are blocked for both P and AP alignments and thus the corresponding conductance is almost zero. There exists a wide

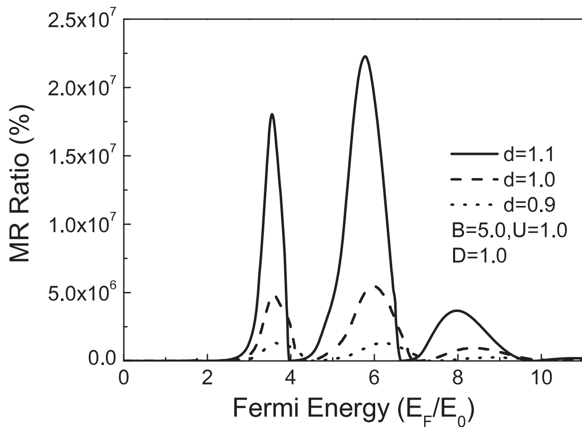

Figure 4. The MR ratio versus Fermi energy. The structural parameters are taken as $B = 5.0$, $U = 1.0$ and $D = 1.0$, where the widths of the stripes are taken as: $d = 0.9$ (dotted curve), $d = 1.0$ (dashed curve) and $d = 1.1$ (solid curve).

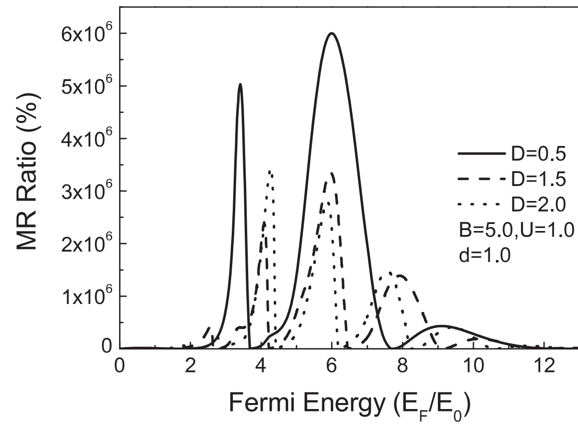

Figure 5. The MR ratio as a function of Fermi energy for different spaces between two stripes: $D = 0.5$ (solid curve), $D = 1.5$ (dashed curve) and $D = 2.0$ (dotted curve). The other parameters are taken as $B = 5.0$, $U = 1.0$ and $d = 1.0$.

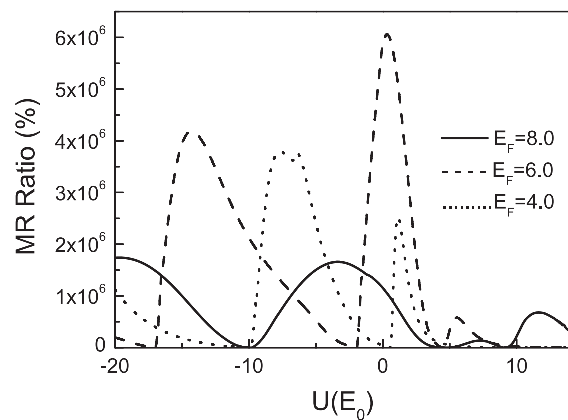

Figure 6. The MR ratio versus the electric barrier U provided by the SM stripe for three fixed Fermi energies $E_{\mathrm{F}} = 4$ (dotted line), $E_{\mathrm{F}} = 6$ (dashed line) and $E_{\mathrm{F}} = 8$ (solid line).

energy region where G_{AP} is closed to zero whereas G_{P} is finite as the blocking effect is more obvious for the AP alignment. Beyond the transmission-blocked region, G_{P} increases rapidly with increasing Fermi energy. Additionally, due to the sharp transmission peaks in the resonance tunneling region, one can see a striking conductance peak with a large peak-to-valley ratio as well as several small peaks in the G_{P}–E_{F} curve. For the AP configuration, there also exists a sharp conductance peak. However, it decays rapidly to zero in the vicinity of this peak. There are also several weak peaks within the transmission-blocked region in the G_{AP}–E_{F} curve. To see the discrepancy between G_{P} and G_{AP} more clearly, in the inset of figure 3 we present the magnetoresistance ratio as a function of the Fermi energy E_{F} for the considered system. A considerable GMR effect can be evidently seen, especially in the low-energy region. It is remarkable that the MR ratio shows drastic oscillations with Fermi energy. In particular, it is striking that the MR ratio can be up to $10^6\%$ at certain low E_{F} and it almost reduces to zero at large Fermi energy. The high values of the MR ratio are due to its definition, since it contains in its denominator G_{AP}, which is much smaller than G_{P}, but the physical reason is the suppression of transmission in the case of AP alignment.

To show the influence of the structural parameters on the GMR effect in our considered device, figure 4 shows the MR ratio versus the Fermi energy for the width of the stripes $d = 0.9$ (dotted curve), 1.0 (dashed curve) and 1.1 (solid curve). It is obvious that the MR ratio depends strongly on the width of the stripes. With d increasing, the MR ratio increases rapidly and the curve slightly shifts towards the low-energy region. In figure 5, we present the MR ratio as a function of the Fermi energy for the space between the stripes $D = 0.5$ (solid curve), $D = 1.5$ (dashed curve) and $D = 2.0$ (dotted curve). Evidently, the MR ratio is strongly correlated with the space between the stripes and the maximum value of the MR ratio reduces rapidly when the space D becomes large. These effects of the structural parameters on the MR ratio of the device are attributed to the variation of its effective potential U_{eff} because the parameters of the stripes greatly influence the profile of the magnetic field (see equation (1)). At the same time, these features also imply that one can greatly enlarge the MR ratio of the device by means of proper fabrication of the stripes in the system.

From the point of view of applications, a controlled MR ratio is desirable for the GMR devices. Now, we explore the tunability of the GMR effect by changing the electric-barrier height (i.e. the applied voltage to the metallic SM stripes in the device considered here). We have calculated the MR ratio as a function of the electric-barrier height U for three fixed Fermi energies: $E_{\mathrm{F}} = 8$ (solid line), 6 (dashed line) and 4 (dotted line), as presented in figure 6. From these three MR curves one can observe that the MR ratio may exhibits a drastic variation with changing the electric-barrier height. The value of the MR ratio greatly varies with the electric-barrier height for certain fixed Fermi energies. Another observation from this figure is that, with increasing E_{F}, the curve shifts rightwards and its peaks broaden. These features originate from the dependence of the effective potential U_{eff} on the electric-barrier height U. Because of the electric barrier induced by an applied voltage to the metallic SM stripes in the system, one can expect that the MR ratio is tuned by adjusting this applied voltage, which may result in a controlled-voltage GMR device.

Finally, we would like to point out that all results presented so far are obtained for the zero-temperature case. It is interesting from the viewpoint of practical applications to know the temperature dependence of the results. As investigated by Papp and Peeters, the effect of temperature is (i) to shift the peaks in the MR ratio to lower Fermi energy and (ii) to broaden and eventually (for $T \gg 1$ K) cause those peaks to completely disappear [17]. In addition, it should be noticed that the phenomenon observed by us in this work is different from the situation in conventional GMR devices, because normally GMR refers to magnetic metallic multilayers. Our observed phenomenon is another kind of MR. In order to differentiate GMR devices in the conventional sense one should call this kind of MR in our proposed device a GMR-like effect or large magnetoresistance (LMR) effect [15].

4. Conclusions

In summary, we propose a GMR device, which can be experimentally realized by the deposition of two parallel FM stripes and a SM stripe on the top of a GaAs heterostructure. We have theoretically investigated the GMR effect in this device and the influence of structural parameters and the applied voltage to the metallic SM stripe on the MR ratio. Our calculations show that the device possesses a considerable GMR effect and its MR ratio is high up to 10^6% at certain energies. The GMR effect results from the evident tunneling difference of electrons in the P and AP configurations, especially the large suppression of transmission for the AP alignment. We have also shown that the MR ratio depends strongly on not only the width of the stripes and the space between the stripes but also the electric-barrier height induced by the applied voltage to the metallic SM stripe. Thus, the MR ratio of the device can be changed by adjusting the locations of the stripes and the applied voltage. Therefore, our proposed device in this work can be used as a tunable GMR device.

References

[1] Baibich M N, Broto J M, Fert A, Nguyen Van Dau F, Petroff F, Etienne P, Creuzet G, Friederich A and Chazelas J 1988 *Phys. Rev. Lett.* **61** 2472

[2] Binasch G, Grunberg P and Zinn W 1989 *Phys. Rev.* B **39** 4828

[3] Prinz G A 1995 *Phys. Today* **48** 58
Prinz G A 1998 *Science* **282** 1660

[4] Heide C 1999 *Phys. Rev.* B **60** 2571

[5] Papp G and Peeters F M 2001 *Appl. Phys. Lett.* **78** 2184

[6] Xu H Z and Okada Y 2001 *Appl. Phys. Lett.* **79** 3119

[7] Peeters F M and Matulis A 1993 *Phys. Rev.* B **48** 15166
Matulis A, Peeters F M and Vasilopoulos P 1994 *Phys. Rev. Lett.* **72** 1518

[8] Zhai F and Xu H Q 2004 *Phys. Rev.* B **70** 085308
Dobrovolsky V N, Sheka D I and Chernyachuk B V 1998 *Surf. Sci.* **397** 333
Guo Y, Gu B, Zong Z, Yu J and Kawazone Y 2000 *Phys. Rev.* B **62** 2635

[9] Ibrahim I S and Peeters F M 1995 *Phys. Rev.* B **52** 17321
Krakovsky A 1996 *Phys. Rev.* B **53** 8469

[10] Kubrak V, Rahman F, Gallagher B L, Main P C, Henini M, Marrows C H and Howson M A 1999 *Appl. Phys. Lett.* **74** 2507
Matulis A and Peeters F M 2000 *Phys. Rev.* B **62** 91

[11] Nogaret A, Carlton S, Gallagher B L, Main P C, Henini M, Wirtz R, NewBury R, Howson M A and Beaumont S P 1997 *Phys. Rev.* B **55** 16037

[12] Overend N, Nogaret A, Gallagher B L, Main P C, Henini M, Marrows C H, Howson M A and Beaumount S P 1998 *Appl. Phys. Lett.* **72** 1724

[13] Edmonds K W, Gallagher B L, Main P C, Overend N, Wirtz R, Nogaret A, Henini M, Marrows C H, Hickey B J and Thoms S 2001 *Phys. Rev.* B **64** 041303

[14] Zhai F, Guo Y and Gu B L 2002 *Phys. Rev.* B **66** 125305

[15] Lu M W and Zhang L D 2003 *J. Phys.: Condens. Matter* **15** 1267
Kong Y H *et al* 2007 *Solid State Commun.* **142** 143
Tang W H *et al* 2007 *Phys. Lett.* A **366** 362

[16] Yang X D, Wang R Z, Guo Y, Yang W, Yu D B, Wang B and Yan H 2004 *Phys. Rev.* B **70** 115303

[17] Papp G and Peeters F M 2005 *Physica* E **25** 339

[18] Papp G and Peeters F M 2004 *J. Phys.: Condens. Matter* **16** 8275
Papp G and Peeters F M 2006 *J. Appl. Phys.* **100** 043707

[19] Lu M W and Yang G J 2007 *Phys. Lett.* A **362** 489
Lu M W and Yang G J 2007 *Solid State Commun.* **141** 248

[20] Kubrak V, Rahman F, Gallagher B L, Main P C, Henini M, Marrows C H and Howson M A 1999 *Appl. Phys. Lett.* **74** 2507
Vančura T, Ihn T, Broderick S, Ensslin K, Wegscheider W and Bichler M 2000 *Phys. Rev.* B **62** 5074

[21] Buttiker M 1986 *Phys. Rev. Lett.* **57** 1761